

Wide Range of Functionalized Poly(*N*-alkyl acrylamide)-based Amphiphilic Polymer Conetworks via Active Ester Precursors

Sebastian Ulrich,^{‡,§} Amin Sadeghpour,^{§,||} René M. Rossi,[‡] Nico Bruns,^{,§} Luciano F. Boesel^{*,‡}*

[‡] Empa, Swiss Federal Laboratories for Materials Science and Technology, Laboratory for Biomimetic Membranes and Textiles, Lerchenfeldstrasse 5, 9014 St. Gallen, Switzerland

[§] Adolphe Merkle Institute, University of Fribourg, Chemin des Verdiers 4, 1700 Fribourg, Switzerland

^{||} Empa, Swiss Federal Laboratories for Materials Science and Technology, Center for X-ray Analytics, Lerchenfeldstrasse 5, 9014 St. Gallen, Switzerland

KEYWORDS. Amphiphilic gels, photopolymerization, pentafluorophenyl acrylate, active ester, nanophase separation, post polymerization functionalization, conetworks, responsive materials, amphiphilic polymer conetwork

ABSTRACT

A versatile strategy for the fabrication of functional and nanostructured poly(*N*-alkyl acrylamide)-based amphiphilic polymer conetworks (APCNs) from hydrophobic precursor networks is presented. The active ester monomer pentafluorophenyl acrylate (PFPA) acts as a general hydrophobic masking group for *N*-alkyl acrylamides, by providing both miscibility with hydrophobic macromonomer crosslinkers and activating the acrylate for amidation reactions. Thereby, hydrophobic precursor networks can be transformed into a multitude of different poly(*N*-alkyl acrylamide)-*l*-PDMS APCNs. The resulting optically transparent APCNs possess nanophase-separated morphologies with domains sizes in the nanometer range. Variation of the amide type results in different types of APCNs, despite them being derived from the same precursor network and having identical network structures. Accordingly, the properties of these APCNs can be tailored according to the desired application by simple variation of the amide functionality. Furthermore, the combination of PFPA with another hydrophobically masked monomer allows for the fabrication of APCNs with small yet precisely defined amounts of functional amide units in the hydrophilic phase. A controlled functionalization of APCNs with pendant groups such as pH-responsive imidazole, fluorescent dyes, and biotin for specific protein binding is achieved, greatly expanding the functionality of the APCNs. Such functionalized APCNs could find application as stimuli-responsive drug delivery membranes, smart hydrogels, biosensors, or as matrices for biocatalysis.

INTRODUCTION

Materials consisting of two types of finely phase separated polymers often possess improved or even novel properties due to a synergistic combination of the individual components in one nanostructured material.¹ Amphiphilic polymer conetworks (APCNs) represent an outstanding class of materials within this field as they combine two polymers of opposite “philicities”, one hydrophilic and one hydrophobic, in a nanophase-separated material.²⁻⁴ Such a phase morphology with domain sizes in the nanometer range results in an extremely large interfacial area and unique properties, such as their ability to swell in both water and hydrocarbons, optical transparency, and excellent mechanical properties. In addition to their most well-known use as silicone hydrogel contact lenses,⁵⁻⁶ the unique set of properties of APCNs make them prime material candidates for applications including drug delivery,⁷⁻¹⁶ anti-biofouling surfaces,¹⁷⁻¹⁹ separation membranes,²⁰⁻²³, lithium ion conduction,²⁴⁻²⁶ sensors,²⁷⁻³¹ self-sealing breathable membranes,³² and matrices for (bio)catalysis.^{31, 33-38} Modification with stimuli-responsive groups adds further layers of functionality and, thereby, opens up new potential applications, which has been shown, for example, with spiropyran-modified APCNs that enabled light-responsive permeation for controlled drug delivery.³⁹

The challenge for the fabrication of APCNs lies within the necessity to combine two immiscible polymers into a macroscopically homogeneous material. Synthetic strategies are typically based on either crosslinking of preformed polymer segments,^{26, 40-50} sequential living polymerization and crosslinking,⁵¹⁻⁵⁶ or the polymerization of hydrophilic monomers with hydrophobic macromonomer crosslinkers,^{15-16, 22, 57-67} with the last one representing the historically most employed approach. All strategies result in conetwork structures where covalent bonds inhibit macro phase separation. However, the use of amphiphilic solvents is usually required to provide miscibility of the components during the conetwork preparation, if it

is possible at all, with one exemption: The use of hydrophilic monomers, bearing highly hydrophobic masking groups, allows for the combination with even extremely hydrophobic macromonomers, while enabling polymerizations in bulk or with very little solvent addition.^{15, 22, 57-62, 68} For example, 2-hydroxyethylacrylate (HEA) was made miscible with a dimethacrylate-terminated poly(dimethylsiloxane) (MA-PDMS-MA) by modification of its hydroxy group with the hydrophobic trimethylsilyl (TMS) group. The masking group was cleaved off after the polymerization, leaving behind an APCN with a hydrophilic poly(HEA) and a hydrophobic PDMS phase.⁵⁸ However, this approach is limited to those hydrophilic monomers with a functional group that can be linked to a suitable masking group. This limitation excludes many monomers, especially members of the extremely versatile class of poly(*N*-alkyl acrylamide)s (PNAAm), which are difficult to incorporate into APCNs. Moreover, each type of masked monomer needs to be individually synthesized, which strongly limits the scope and variability of accessible materials.

Beyond the fabrication of APCNs, the functionalization of APCNs is an important step towards many applications, however, it faces closely related challenges:³⁹ post-polymerization functionalization requires the presence of adequate functional groups in the APCNs and the degree of functionalization is, typically, not well controlled. Incorporation via functional monomers, on the other hand, is limited by miscibility restrictions since many of the molecules of interest, such as fluorescent dyes or photochroms, are highly hydrophilic. Furthermore, many functional monomers could interfere with the polymerization process or be lost due to side reactions. An ideal synthesis strategy for APCNs would, therefore, involve a monomer which is hydrophobically masked with a group that allows integration into hydrophobic preAPCNs but activates the monomer towards a variety of different post-polymerization functionalizations.

The active ester monomer pentafluorophenyl acrylate (PFPA) offers a solution to this challenge as it combines hydrophobicity with a very high reactivity towards primary but also secondary amines, a reaction that yields *N*-alkyl acrylamide (NAAm) units.⁶⁹ Indeed, PFPA could be considered a hydrophobically masked NAAm, as it can be transformed into many different members of this wide-ranging class of monomers. Since its introduction together with the less reactive pentafluorophenyl methacrylate by Théato and coworkers,⁷⁰ PFPA has been employed for the preparation of various PNAAm- and ester-based systems,⁷¹ such as blockcopolymers,⁷²⁻⁷⁴ nanohydrogels,⁷⁵⁻⁷⁷ functional surfaces,⁷⁸⁻⁸¹ and visible light responsive polymer films and polymersome nanoreactors.⁸²⁻⁸³

Herein, we describe the synthesis of APCNs via hydrophobic preAPCNs based on PFPA and PDMS macromonomers. A variety of different PNAAm/PDMS APCNs were prepared from one preAPCN and characterized using an array of analytical techniques. Furthermore, mixed preAPCNs based on PDMS, defined amounts of PFPA and the well-established TMS-masked HEA provided access to poly(HEA)-*l*-PDMS APCNs that were modified with a defined amount of functional groups, such as pH-responsive imidazole groups, fluorescent dyes, and biotin for specific protein binding. Thereby, a synthetic platform for the creation of a wide range of functional APCNs is established.

EXPERIMENTAL SECTION

Materials. All solvents including anhydrous solvents were purchased from Sigma Aldrich or Fisher Scientific and were of analytical grade. Other reagents, if not stated otherwise, were purchased from Sigma Aldrich (Switzerland) or TCI Europe (Germany). Streptavidin AlexaFluor488 conjugate was purchased from Thermofisher (Switzerland). Polypropylene tape (50 μm thickness, Tesa, Germany) was purchased from Distrelec (Switzerland). Sterile

Dulbecco's Phosphate Buffered Saline (PBS) was purchased from Sigma Aldrich. Methacryloxypropyl-terminated poly(dimethylsiloxane) (MA-PDMS-MA, viscosity 50-90 cSt., 4500-5500 g mol⁻¹; ¹H-NMR: M_n = 4600 g mol⁻¹; GPC: M_n = 3500 g mol⁻¹; PDI = 1.7) was purchased from ABCR (Germany). Britton-Robinson "universal" buffer (range pH 2-12) was prepared according to a literature procedure,⁸⁴ and adjusted to the required pH values with 0.5 M NaOH. PFPA and TMS-HEA were prepared according to previously reported procedures and stored under argon at -20 °C until use.^{58, 72}

Synthesis of preAPCN. Detailed compositions of the monomer mixtures are provided in the Supporting Information (**Table S1**). In a typical procedure, photoinitiator Irgacure 651 was dissolved in TMS-HEA or, for PFPA-49, in THF (25 vol%) followed by the addition of PFPA and MA-PDMS-MA (0.6 mL, 0.59 g). The monomer mix was vortexed (30 s) and placed in an ultrasonication bath (30 s). A glass slide equipped on two sides with approximately 200 μm spacers (4 layers of 50 μm thick polypropylene tape) was covered with the monomer mixture. A glass slide without spacers was placed on top and the mixture, which was then photopolymerized in a UV chamber (UVASPOT 400/T, 400 W, 315 nm long pass filter, Dr. Hönle AG, Germany) for 3 min from each side. The glass slides were subsequently placed in acetone to facilitate separation of the conetworks from the glass slide. The conetworks were removed, washed for several hours in THF (40 °C) and dried on a filter paper under vacuum to yield optically transparent preAPCNs of 170-200 μm thickness.

Synthesis of APCN. Detailed amounts of reagents for the conversion of the PFPA active esters in preAPCNs into *N*-alkyl acrylamide units are provided in the Supporting Information. Typically, the preAPCNs (2-5 cm²) were placed in 10 mL THF, THF/DMSO (2:1), or DMF in a screw cap glass vial. The amines and triethylamine (TEA) as an auxiliary base were added, the

vial was closed and the reaction was allowed to proceed on a shaker (160 rpm) at 40 °C overnight or, for DMF, 1 h. Subsequently, the conetworks were washed in THF, acetone and ethanol. Conetworks containing TMS-HEA were placed in an acidified water/*i*-propanol mixture (16 drops 37 % HCl per liter) overnight and, subsequently, washed in THF overnight, acetone for several hours, and ethanol overnight. The samples were dried on a filter paper under vacuum to yield optically transparent APCNs of 160-200 μm thickness.

Swelling Measurements. Dry samples of 1-2 cm² were immersed into water or *n*-heptane for at least one night. The edge lengths L_i before and after swelling were measured with an optical microscope (Keyence VHX-1000 system) and the average volumetric degree of swelling S_{Vol} was subsequently determined from the sample edges (length L) as

$$S_{Vol} = \frac{1}{n} \sum_{i=1}^n \left(\frac{L_{i,swollen}}{L_{i,dry}} \right)^3$$

with n denoting the number of edges. Typically, 4 edges were used, unless an edge was damaged or too short and could not be measured. For swelling experiments of pH responsive APCNs, samples were immersed in universal buffer solutions (Britton-Robinson buffer) at pH 2, 4, 6, or 8 overnight and S_{Vol} was determined. Cycling experiments were conducted by switching a single sample between buffer solutions of pH 4 and 8, respectively. For each step, the APCN was allowed to equilibrate for at least one day.

AlexaFluor488-Streptavidin Loading. For the loading with proteins, Biotin 0.1 and *n*-BA-0.1 were cut into easily distinguishable shapes and incubated together in 2 mL sterile PBS buffer containing 0.5 mg/mL of AlexaFluor488-streptavidin conjugate for one night. The conetworks were transferred to 10 mL fresh sterile PBS buffer and fluorescence intensity values were determined immediately within 10 min. The conetworks were kept in 10 mL PBS buffer with

fluorescence intensity measurements after 1, 2, 6, and 37 days with an exchange of the PBS buffer solution before any measurements.

Infrared (IR) Spectroscopy. Attenuated total reflectance Fourier transform infrared (ATR FT-IR) spectra were recorded on a Varian 640-IR FT-IR (Agilent Technologies) spectrometer on the sample surface or, for bulk measurements, on powders obtained with a cryomill (CryoMill, Retsch, Germany).

Gel permeation chromatography (GPC). GPC was measured on an Agilent 1100 Series HPLC (Agilent, USA, serial coupled columns: PSS SDV 5, 100A, PSS SDV 5, refractive index and diode array detector at 235 and 254 nm) with THF as the mobile phase (flow rate: 1 mL min⁻¹, temperature: 30 °C), calibration on PDMS standards and toluene as the internal standard.

Differential Scanning Calorimetry (DSC). DSC curves were recorded on a NETZSCH DSC 214 Polyma (NETZSCH, Germany) under nitrogen atmosphere at a heating rate of 10 K min⁻¹ and analyzed using the associated software (NETZSCH Proteus Thermal Analysis, Version 7.1.0). Due to swelling of the APCNs with atmospheric water, glass transition temperatures were determined for the second heating cycle as the middle point of the observed transitions.

Atomic Force Microscopy (AFM). AFM analysis was conducted on a scanning probe microscope FlexAFM V5 (Nanosurf AG, Switzerland) equipped with a C3000 controller and the associated software (Nanosurf C3000 Version 3.7.3.6). Measurements were performed at ambient conditions in tapping mode with a silicon AFM probe (Tap-150Al-G, BudgetSensors, Bulgaria) with a force constant of 5 N m⁻¹ and resonance frequency of 150 kHz. Images were obtained on dry samples on the sample surfaces or on cross sections, with the latter obtained by cryo fractures in liquid nitrogen or from cuts with a microtome-type blade. The data was analyzed using Gwyddion software (Version 2.46).

Small Angle X-ray Scattering (SAXS). SAXS studies were carried out using a Nanostar SAXS instrument (Brucker AXS GmbH, Karlsruhe, Germany). The instrument is equipped with a microfocussed X-ray source (Incoatec GmbH, Geesthacht, Germany) providing Cu K α radiation and MONTEL optics with two pinholes of 300 μm to focus the X-ray beam. A VÅNTEC-2000, Xe-based gas avalanche detector was used to record the 2D scattering patterns. The scattering patterns of dry samples were recorded over 30 minutes of exposure time at room temperature. The scattering intensities as a function of scattering vector ($q = \frac{4\pi}{\lambda} \sin(\theta)$) were obtained by azimuthal integration of 2D patterns and were further considered for detailed structural analysis of the nanodomains. The generalized indirect Fourier transformation approach was applied to obtain information about the size of the domains and their spatial correlations (form factor and structure factor calculations).⁸⁵⁻⁸⁶ As the result, the average size of the domain (pair-distance distribution function) and their spacing (domain-domain correlations) have been identified.

Energy Dispersive X-ray Spectroscopy (EDX). EDX analysis was performed on a Hitachi S-4800 (Hitachi High technologies, Canada) at 20 eV. Samples were first sputter coated with 5 nm gold/palladium on a SEM coating unit (Polaron Equipment, E5100, Kontron AG, Switzerland). Silicon and carbon signals were compared relative to the respective number of atoms per repeating unit.

Fluorescence Measurements. For fluorescence intensity quantification, wet samples were placed between two glass slides and analyzed in a fluorescence microarray scanner (LS ReloadedTM, Tecan Trading AG, Switzerland, 100 μm height, 130 gain). Fluorescence intensity values were determined over the APCN area via ImageJ (Version 1.51n) and subtracted by the background value. Fluorescence spectra of APCNs were recorded on a Cary Eclipse fluorescence

spectrophotometer (Agilent, USA) on wet or dry samples. EDANS-0.1 and respective control: Excitation spectra: λ_{Exc} 200-450 nm, λ_{Em} = 480 nm, ex. and em. slit 2.5 nm. Emission spectra: λ_{Exc} 335 nm, λ_{Em} = 380-700 nm. ex. and em. slit 2.5 nm. Biotin-0.1 and respective control: λ_{Exc} = 488 nm, λ_{Em} = 500-650 nm ex. and em. slit 10 nm.

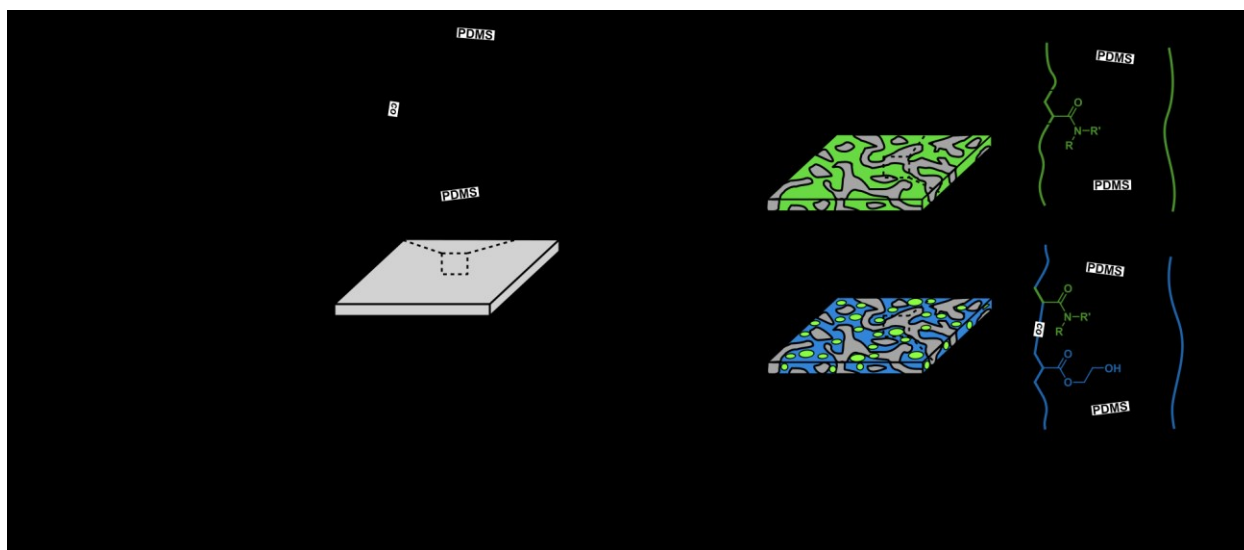


Figure 1. (a) Synthetic procedure for the fabrication of PNAAm-based APCNs via hydrophobic preAPCNs based on PFPA, MA-PDMS-MA and TMS-HEA. Depending on the monomer ratio, the final composition of APCNs range from PNAAm/PDMS systems (right, top) to HEA-based APCNs with defined amounts of functional NAAM units (right, bottom). Reaction conditions: (i) photopolymerization (bulk or 25 vol% THF for PFPA-49, UV irradiation, 315 nm long pass filter), (ii) R-NH₂, TEA, THF or THF/DMSO (40 °C, overnight), or DMF (40 °C, 1 h) and, if TMS-HEA was incorporated, (iii) acidified *i*-PrOH/H₂O 1:1 (room temperature, overnight). (b) Primary and secondary amines used to introduce the NAAM units into APCNs.

Table 1. Synthesized conetworks and their composition.

Sample	Composition (mol%) ^a	Composition (wt%) ^b
PFPA-49	49/0/51	75/0/25
PFPA-5	5/44/51	9/63/29
PFPA-0.1	0.1/48.8/51.1	69.6/1.5/28.9
AEE-49	49/0/51	67/0/33
HPA-49	49/0/51	63/0/37
Morph-49	49/0/51	65/0/35
DMAPA-49	49/0/51	67/0/33
Hist-5	5/44/51	8/53/39
EDANS-0.1	0.1/48.8/51.1	0.3/59.8/39.9
Biotin-0.1	0.1/48.8/51.1	0.4/59.7/39.9
n-BA-0.1	0.1/48.8/51.1	0.1/59.9/40.0
HEA-49	0/50/50	0/60/40

^a theoretical molar ratio of repeating units calculated from monomer feed: PFPA/TMS-HEA/dimethylsiloxane or NAAm/HEA/dimethylsiloxane. ^b theoretical weight composition.

RESULTS AND DISCUSSION

Design and Synthesis. The general strategy for the synthesis of PFPA-based APCNs is provided in **Figure 1a**. In short, PFPA, TMS-HEA, the macromonomeric crosslinker MA-PDMS-MA, and photoinitiator Irgacure 651 were mixed. The monomer mixture was photopolymerized between two glass slides equipped with 200 μm spacers by UV irradiation (**Figure S1**). The polymerization resulted in free standing hydrophobic preAPCNs that consisted of random copolymers crosslinked by PDMS chains: poly((PFPA-*co*-TMS-HEA)-*l*-PDMS). The amount of PFPA in the conetworks depended on the initial monomer ratio and could be chosen all the way up to preAPCNs consisting of only PFPA and PDMS: poly(PFPA-*l*-PDMS). Here,

however, a small amount of THF (25 vol% of PFPA) was needed to ensure full miscibility. The synthesized preAPCNs are listed in **Table 1** (top) with their theoretical molar and weight compositions. Molar compositions are given for the ratios between individual repeating units, i.e. PFPA, TMS-HEA or the dimethylsiloxane units of PDMS. To demonstrate the wide range of accessible compositions, we synthesized preAPCNs with 49 mol% of PFPA for entirely PNAAm-based APCNs (PFPA-49) as well as preAPCNs with 5 mol% (PFPA-5) and 0.1 mol% (PFPA-0.1) for HEA-based APCNs with different degrees of functionalization. PFPA-49 was chosen to allow the investigation of APCNs with a hydrophilic phase with only one type of repeating unit. With PFPA-5, a degree of functionalization is introduced that should be sufficient to change bulk properties. PFPA-0.1, on the other hand, allows the controlled introduction of groups, for example fluorescent dyes, that function at very low concentrations. In addition, preAPCNs with a 0.2:1 and a 1:1 ratio of PFPA to HEA units (0.2:1 and 1:1) and a higher amount of PDMS and the resulting APCNs are described in the Supporting Information.

Reaction of the active ester with primary or secondary amines transformed PFPA-49 into APCNs with the network structure poly(NAAm-*l*-PDMS), in which hydrophilic poly(NAAm) segments are connected by the hydrophobic PDMS chains (**Figure 1a**). For PFPA-5 and PFPA-0.1, the active ester reaction was followed by cleavage of the TMS group, resulting in APCNs with the structure poly(NAAm-*co*-HEA)-*l*-PDMS). The primary and secondary amines employed in this work are depicted in **Figure 1b**. They were 2-hydroxypropylamine (HPA), 2-(2-aminoethoxy)ethanol (AEE), morpholine (Morph), and *n*-butylamine (*n*-BA). The amines were chosen due to the distinct differences in their chemical structure: HPA and AEE result in a protic secondary amide though AEE brings a longer amide side chain with a primary alcohol and an additional ether group. Morpholine, in contrast, results in an aprotic and less hydrophilic

tertiary amide with a ring structure. Moreover, two amines bearing pH-responsive side groups, 3-(dimethylamino)propyl-1-amine (DMAPA) and histamine (Hist), were used, as well as the fluorescent dye (5-((2-aminoethyl)amino)naphthalene-1-sulfonic acid) (EDANS) and an amine-modified biotin (Biotin-NH₂). The *n*-BA was used for control experiments. Due to the excellent reactivity of PFPA active esters, mild reaction conditions (THF, 40 °C) could be employed for the amidation reaction.⁷⁰ For amines with low solubility in THF, either DMSO was added (Hist) or the reaction was conducted in DMF (EDANS, Biotin-NH₂). Due to the higher reactivity of PFPA in DMF, the reaction time was shortened to one hour.⁸⁷ Cleavage of the TMS groups to liberate the hydrophilic HEA units took place under mild conditions in an acidified water/isopropanol mixture. The synthesized APCNs are listed in **Table 1** (middle). Importantly, from one preAPCN, several different APCNs could be synthesized. For example, from preACPN PFPA-49, which contains only PFPA and PDMS, all PNAAm-based APCNs were derived, whereas both fluorescently-labeled EDANS-0.1 and Biotin-0.1 as well as the *n*-BA-modified, *n*-BA-0.1 were derived from **PFPA-0.1**. For comparison, we also synthesized HEA-49 which only contained poly(HEA) and PDMS (**Table 1**, bottom).

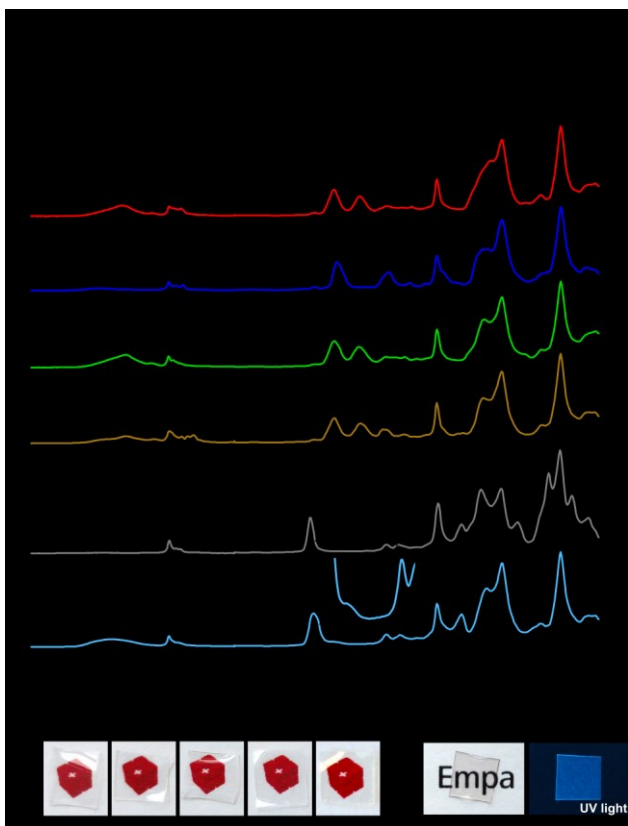


Figure 2. (a) Surface attenuated total reflectance Fourier transform infrared (ATR FT-IR) spectra of preAPCNs **PFPA-49** and **PFPA-0.1**, as well as APCNs derived from them. (b) Photographic images of (left-to-right) **PFPA-49**, **AEE-49**, **Morph-49**, **HPA-49**, and **DMAPA-49** (c) Photographic images of fluorescent **EDANS-0.1** under daylight and under near-UV irradiation.

Incorporation of PFPA into the preAPCNs and the reaction of the PFPA active esters could be conveniently analyzed by IR spectroscopy due to the strong and characteristic signals of the PFPA active ester group (1782 cm^{-1}) and the aromatic C-F bond (1516 cm^{-1}).⁸² FT-IR spectra of PFPA-49 and several PNAAm-based APCNs that were derived from it (AEE-49, Morph-49, HPA-49, DMAPA-49) are presented in **Figure 2a**. Reaction of the PFPA active ester and

formation of the corresponding amide were accompanied by loss of the PFP ester signals and of the aromatic C-F bond signal indicating complete conversion. The formation of the amides resulted in the appearance of the amide peak around 1640 cm^{-1} and, for secondary amides, an additional peak for the N-H bending vibration at 1545 cm^{-1} . The different chemical nature of the amide units can also be distinguished in the O-H region: as expected, no signal is observable for the hydrophobic PFPA-49, whereas AEE-49 and HPA-49 both possess protic O-H and amide N-H groups resulting in a broad mixed peak with a maximum around 3300 cm^{-1} . The aprotic Morph-49 shows a weak O-H signal, most likely caused by atmospheric water vapor due to the hygroscopic nature of the PNAAm phase. For DMAPA-49 a stronger water O-H signal is combined with the amide N-H peak. Bulk IR spectra were recorded on cryomilled samples and confirmed complete reaction throughout the conetwork and showed only minor differences between surface and bulk (**Figure S2**).

APCNs with a hydrophilic phase based on HEA but a small amount of amide modification are available, for example the APCN EDANS-0.1 from preAPCN PFPA-0.1. The FT-IR spectra of both networks are presented in **Figure 2a** (bottom). At this low concentration, the PFP ester peak was too small to be observed, however, the stronger aromatic C-F peak could still be used to confirm the incorporation of PFPA and the successful transformation into the amide (**Figure 2a**, insets). The disappearance of the peak corresponding to the TMS group at 837 cm^{-1} and the corresponding appearance of the typical alcohol O-H peak around 3400 cm^{-1} confirmed the complete cleavage of the TMS masking groups from the HEA units. FT-IR spectra of the other preAPCNs and APCNs of **Table 1** can be found in the supporting information (**Figure S3-7**). All preAPCNs and APCNs appeared transparent to the eye (photographic images in **Figure 2b**), indicating that no macroscopic phase separation had taken place, i.e. domain sizes were below

the light scattering limit in the nanometer range. The presence of the fluorescent dye in EDANS-0.1 resulted in a very light reddish color in daylight and strong blue fluorescence under near-UV irradiation (366 nm peak, **Figure 2c**). The dye was homogeneously distributed throughout the APCN. To verify the selective reaction of the EDANS with PFPA, a control experiment was conducted with *n*-BA-0.1. After being treated to the same reaction conditions (EDANS/TEA, DMF, 40°C, 1 h), fluorescence spectroscopy revealed no fluorescence signal for this control sample whereas strong peaks typical for the dye were found for EDANS-0.1. (**Figure S3**).

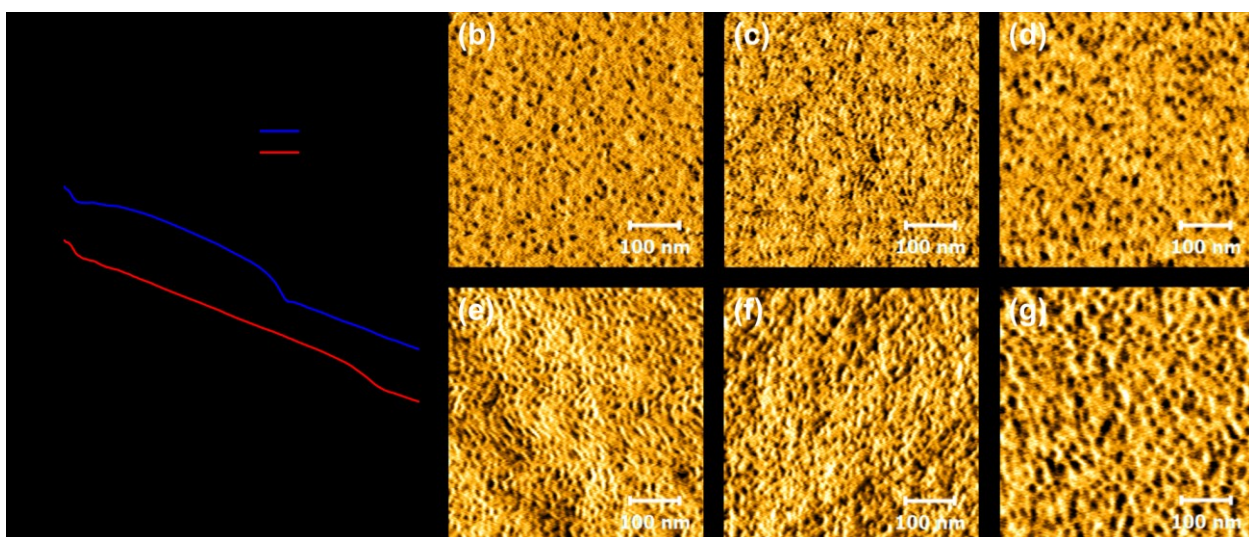


Figure 3. Characterization of the phase morphology of conetworks by DSC and AFM. (a) DSC curves of PFPA-49, AEE-49 and Morph-49. The glass transitions are marked by arrows. (b-g) Phase mode AFM images of surfaces (b-d) and cross sections (e-g) of dry samples: AEE-49 (left), Morph-49 (middle), EDANS-0.1 (right).

Thermal Analysis. Phase separation in APCNs typically results in two distinct glass transition temperatures (T_g) corresponding to the hydrophilic and hydrophobic phase, respectively, which can be observed by differential scanning calorimetry (DSC).⁵⁸ All APCNs were analyzed by DSC. The DSC curves of preAPCN PFPA-49, the protic APCN AEE-49, and the aprotic APCN Morph-49 are presented in **Figure 3a**. The T_g of the other APCNs are listed in **Table S2**. Interestingly, not only the final APCNs but also the all-hydrophobic PFPA-49 possessed two T_g , indicating that poly(PFPA) and PDMS became immiscible during the polymerization. They phase-separated on the nanometer scale since no macrophase separation was observed that would turn the networks opaque. All conetworks have the same PDMS phase that corresponds to a T_g around -130 °C, however, they differ in the nature of the hydrophilic phase. The second T_g of AEE-49 is 46 °C. The T_g of Morph-49 lies at 124 °C, most likely because of its inflexible cyclic morpholine amide group. Interestingly, for all PNAAm-based APCNs, the second T_g lies above or around room temperature, whereas for HEA-49 and other mostly HEA-based APCNs such as EDANS-0.1 it is around 10 °C. Consequently, the latter materials are much softer at room temperature in the dry state than the other APCNs. Another observation is that APCNs that contain different amounts of HEA and NAAM possess only one T_g for the hydrophilic phase. This result allows to draw the conclusion that the hydrophilic phase is a mixed phase of poly(HEA) and PNAAM. The T_g closely reflects the NAAM/HEA ratio (**Figure S7**) in that, for example, a 1:1 ratio of HEA to HPA-NAAM units results in a T_g of 72 °C, almost in the middle between the T_g s found for a HEA phase (10 °C) and a HPA-NAAM phase (114 °C). In conclusion, the choice of the type of NAAM as well as the ratio of NAAM to HEA strongly influences the T_g of the hydrophilic phase and, therefore, the mechanical properties, especially the softness/stiffness of the APCNs.

Phase Morphology. The phase morphology of the APCNs was investigated by AFM and SAXS. The contrast in phase mode AFM images is related to a difference in energy dissipation, allowing the distinction of harder (bright) and softer (dark) domains.⁸⁸ Phase mode AFM images obtained on surfaces and cross sections of dry samples are presented in **Figure 3b-g** for representative APCNs: the protic AEE-49, the aprotic Morph-49 and the HEA-based EDANS-0.1. Additional AFM images for the other APCNs, as well as a low magnification overview and a related height mode image of AEE-49 can be found in the supporting information (**Figure S5-8**). All images in **Figure 3** clearly show distinct phase separated domains of PDMS on the surfaces and the cross sections. The concentration of PDMS domains on the surfaces is lower than on the cross-sections, which could be related to the contact of the monomer mixture with the hydrophilic glass slide during the polymerization. Most likely, PDMS as the most hydrophobic component has a lower affinity to the glass surface, resulting in an enrichment of the other monomers.⁵⁸ Nevertheless, both phases were present on all surfaces. The PDMS domains of all protic PNAAm-based and HEA-based APCNs appeared mostly round, though less so for Morph-49. The found phase morphology can be interpreted as the presence of distinct, often almost spherical domains of PDMS within a continuous hydrophilic matrix. This observation can be related to the overall composition of the APCNs that contain more than 60 wt.% hydrophilic phase. The diameter of single domains was found predominantly between 5 nm and 12 nm. For EDANS-0.1, the single domains are larger. Most of them had a diameter larger than 10 nm and closely resemble the phase morphology found for HEA-49 (**Figure S6**). This finding indicates that the incorporation of small amounts of functional amides does not influence the phase morphology of HEA-based APCNs.

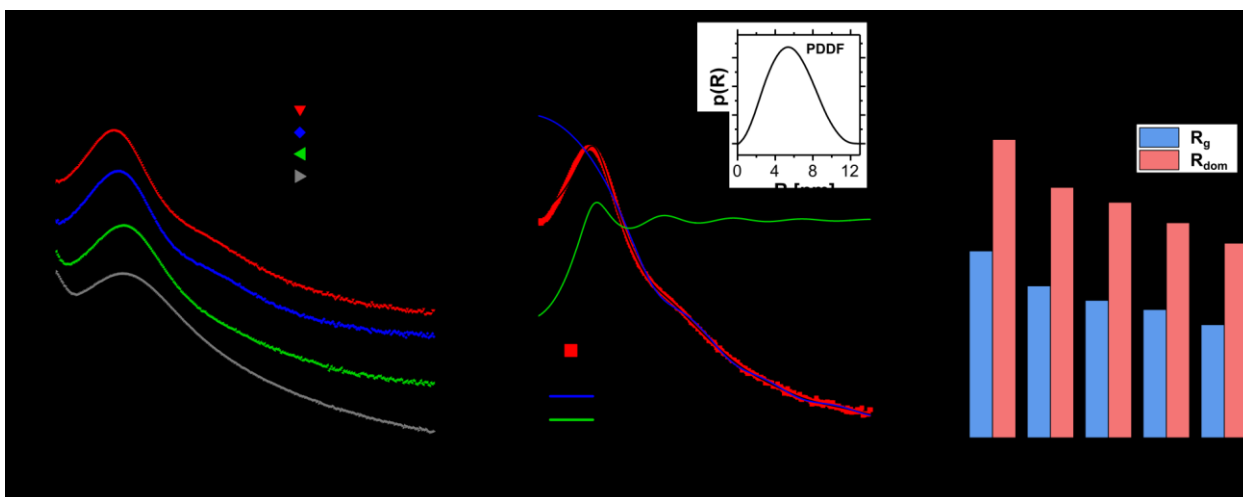


Figure 4. Characterization of the structure of conetworks by SAXS. (a) SAXS profiles obtained from dry samples of PFPA-49 and three ACPNs derived from it, AEE-49, HPA-49, and Morph-49, as well as HEA-49, shifted vertically for comparison. First and second order peaks (q^* and $2q^*$) are marked with arrows where observable. (b) Example GIFT analysis with hard sphere interaction model is shown for AEE-49. The corresponding form factor $P(q)$ and structure factor $S(q)$ as well as the PDDF function (inset) is represented. Hard sphere model fit shown for AEE-49 as an example with corresponding form factor $P(q)$ and structure factor $S(q)$ as well as the PDDF function (inset). (c) Domain sizes (R_g) and domain-domain correlation length radius (R_{dom}) obtained from fitting of the SAXS traces.

SAXS represents a powerful tool to gain further insight into the bulk phase morphology of APCNs and other randomly crosslinked conetworks.^{25-26, 60-61, 89-90} Herein, the influence of the chemical nature of the NAAm units on the phase morphology was of particular interest. The 2D SAXS patterns of the conetworks possessed a continuous ring structure, indicating that the conetworks are randomly oriented as would be expected from the random polymerization process (**Figure S9**). SAXS traces obtained from dry samples of three different PNAAm-based

APCNs, AEE-49, HPA-49, and Morph-49 as well as their precursor conetwork PFPA-49 are presented in **Figure 4a**. The SAXS trace of HEA-49 is also shown for comparison. A scattering peak from domain-domain correlations is observable for all conetworks and confirms the presence of domains in the nanometer range with alternating electron densities and, thus, variations in contrast.⁹¹ Interestingly, the preAPCN PFPA-49 also shows a scattering peak. Thus, the SAXS data confirms the observations from the DSC analysis that PFPA-49 is a nanophase-separated conetwork with distinct domains of poly(PFPA) and of PDMS. The main peak position q^* can be interpreted as an inter-domain spacing. For the APCNs with protic amide units, AEE-49 and HPA-49, as well as HEA-49 with its protic glycol ester, a second order peak was found at $2q^*$, which is more clearly observable in the corresponding Kratky plots (**Figure S9**). The second order peak indicates correlated second nearest neighboring domains due to a short-range order. No higher order diffractions were observed indicating a lack of longer range ordering. Such a finding is typical for covalent conetworks with a randomly crosslinked structure which hinders the development of long-range orders, such as those typically found for self-assembled block copolymers.^{60-61, 92} For the aprotic Morph-49 and the all-hydrophobic PFPA-49, no second order peak ($2q^*$) was found, which may indicate less well-ordered domains or blurry interfaces between alternating regions. To achieve a more quantitative perspective on the nanodomains, the SAXS curves were fitted using the generalized indirect Fourier transformation (GIFT) approach by applying a hard-sphere interaction model. A similar model-based method has been shown before to be able to simulate the SAXS data of similar APCNs.⁶¹ The fit is shown for AEE-49 as an example in **Figure 4b** with the contributions of the form factor $P(q)$ and the structure factor $S(q)$ as well as the corresponding pair-distance distribution function (PDDF). The latter indicates the radius of gyration, R_g , and its almost symmetric shape demonstrates a relatively

monodisperse distribution in the size of domains. Apart from the PDDF which contains the information from the form factor, the radius for the domain-domain correlation length, R_{dom} , can be derived from the structure factor $S(q)$. **Figure 4c** summarizes the results obtained from fitting of the SAXS profiles. HEA-49 has the largest domain size ($R_g = 5.3$ nm) and inter-domain correlation length ($R_{dom} = 8.5$ nm) of all conetworks, whereas the domains of AEE-49, HPA-49 and Morph-49 are smaller ($R_g = 3.7$ - 4.3 nm and $R_{dom} = 6.1$ - 7.1 nm). These findings correspond well to the finer domain structures that were observed in the cross-section AFM images of these conetworks (**Figure 3b/c**, **Figure S8**). It is worth mentioning that the decrease of R_g and R_{dom} from AEE-49 over HPA-49 to Morph-49 and PFPA-49 could be related to the size difference and the chemical characteristics of the *N*-alkyl acrylamide repeating units.

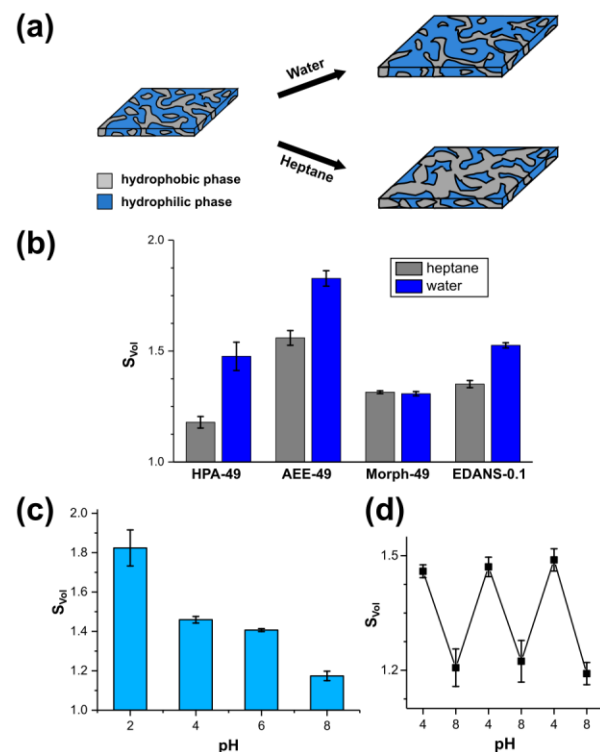


Figure 5. Swelling of APCNs. (a) Schematic depiction of the swelling of the APCN's phases depending on the hydrophobicity/hydrophilicity of the swelling medium. (b) Volumetric degree

of swelling SVol of selected APCNs. (c) Swelling of imidazole-modified APCN Hist-5 in aqueous buffer solutions of different pH and (d) pH cycling of one His-5 specimen. Error bars indicate the variation of SVol calculated from different edges of the samples.

Swelling Behavior. The ability to swell in solvents of highly different polarity is a defining feature of APCNs (**Figure 5a**).³ Therefore, the volumetric degree of swelling S_{Vol} of the various conetworks was measured in water and in the hydrophobic solvent *n*-heptane at room temperature. S_{Vol} is defined as

$$S_{Vol} = \frac{V_{wet}}{V_{dry}}$$

where V_{dry} is the volume of a sample in the dry state and V_{wet} , the volume after swelling to equilibrium in a solvent. **Figure 5b** presents S_{Vol} for the PNAAm-based HPA-49, AEE-49, and Morph-49, as well as for the HEA-based EDANS-0.1. All these materials swell in both solvents, albeit to different extents. The highest swelling in both *n*-heptane and water were found for AEE-49 with S_{Vol} of 1.82 and 1.55, respectively. In contrast, HPA-49 swelled less in both solvents. Interestingly, Morph-49 swelled equally well in *n*-heptane and water (both $S_{Vol} = 1.31$). The swelling behavior of the conetworks supports their character as nanophase-separated APCNs and emphasizes the influence of the chosen *N*-alkyl acrylamide units on the properties of the APCNs. All conetworks have a similar PDMS content and, therefore, a similar hydrophilic to hydrophobic ratio. Furthermore, since all the PNAAm conetworks are derived from the same preAPCN and, thus, possess an almost identical network structure, the differences in water swellability have to arise from different properties of the hydrophilic phase, e.g. its polarity. The strong swelling in water of AEE-49 indicates that the AEE amide is the most hydrophilic one

among the compared samples, which could be related to the larger molecular weight of one repeating unit and the presence of more hydrophilic groups. Morph-49, on the other hand, possesses the least hydrophilic polar phase due to the lack of protic groups, which is mirrored by the weakest swelling in water. With the PDMS constituting the hydrophobic phase of all APCNs, similar swelling in *n*-heptane could be expected, which is clearly not the case. This finding indicates that the properties of the hydrophilic phase influence the swelling of the PDMS phase as well. The stiffness of the hydrophilic phase could mechanically limit the swelling of the PDMS phase for HPA-49 with its T_g of 114 °C. The softer AEE-49, on the other hand, swelled much stronger. Similar observations have been made for other APCNs where stiff high- T_g phases resulted in little swelling of the other phase.⁵⁹ For Morph-49, despite its high T_g , the low hydrophilicity of the amides might allow for some swelling of the hydrophilic phase in *n*-heptane or a plasticizing effect of the solvent. The swelling properties of EDANS-0.1 mirror its composition: clear swelling in both *n*-heptane and water, with the former little restricted by the low- T_g poly(HEA) phase. Swelling in water is higher than in the organic solvent due to the bigger weight fraction of the hydrophilic phase.

Incorporation of pH-responsive side groups into the hydrophilic chains of APCNs should render the swelling behavior of APCNs pH-dependent. DMAPA-49 with its tertiary amine groups swelled strongly in Britton-Robinson buffer of pH 7 ($S_{Vol} = 2.34$). However, the APCN became opaque and white flakes separated from the conetwork within three days of incubation, indicating that the APCN degraded. Most likely, the amine side groups act as nucleophilic catalyst for the hydrolysis of the methacrylate ester end group of the PDMS crosslinker. Imidazole side groups that result from the reaction of PFPA with histamine are also pH-responsive, but less nucleophilic, so that it could be expected that Hist-based APCNs would not

degrade. To further demonstrate that a defined amount of functional units can be incorporated to tailor the APCN's properties, we synthesized Hist-5 from PFPA-5 with 5 mol% of imidazole units overall and 10 mol% of the hydrophilic phase. The imidazole side group has a pK_a of 6.0.⁹³ Therefore, swelling was assessed in buffer solutions from pH 2 to 8 (**Figure 5c**). Depending on the pH of the buffer and, thereby, the protonation of the imidazole groups, Hist-5 showed varying degrees of swelling from 1.17 at pH 8 to 1.82 at pH 2. Furthermore, the pH-responsive swelling was reversible and could be cycled by repeatedly switching the buffer solution for one sample (**Figure 5d**).

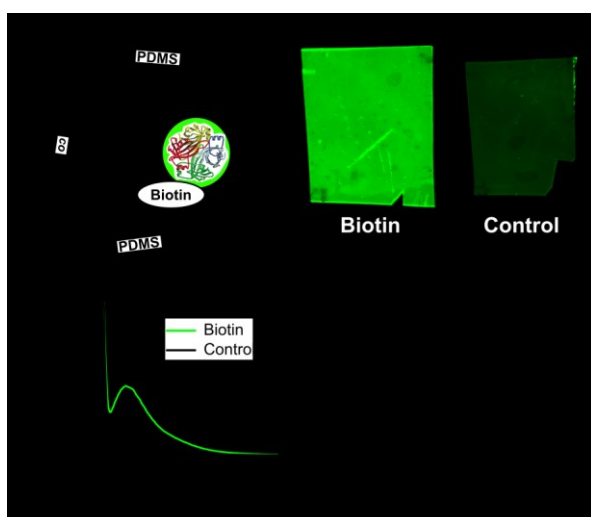


Figure 6. Biotin-modified APCNs for specific binding of proteins. (a) Loading of Biotin-0.1 with fluorescently labeled streptavidin. (b) Fluorescence scanner image of Biotin-0.1 and *n*-BA-0.1 (non-functionalized control) that were incubated with streptavidin AlexaFluor488 conjugate for 1 day and, then, washed for 2 days in PBS. (c) Corresponding fluorescence emission spectra ($\lambda_{Exc} = 488 \text{ nm}$) after 2 days of washing in PBS. (d) Ratio of fluorescence intensities per area unit $I_{biotin}/I_{control}$ taken from such images. Measurements were conducted directly after incubation with fluorescently-labeled streptavidin and after 1, 2, 6 and 37 days of washing in PBS. Error bars were derived from the intensity distribution over the APCN area.

Specific Protein Binding. The loading of proteins and, especially, enzymes into APCNs allows for their application as matrices for biocatalysis and as biosensors.^{28, 33, 35-37, 94} However, if they are to be used in an aqueous environment, the biomacromolecules need to be bound into the APCNs to avoid or reduce leaching. Modification of the conetworks with biotin provides a pathway towards APCNs that bind proteins due to biotin's ability to strongly and specifically bind (strept)avidin and (strept)avidin-labeled proteins, as depicted schematically in **Figure 6a**.⁹⁵ To this means, we reacted PFPA-0.1 with Biotin-NH₂ to create the APCN Biotin-0.1. A control sample, *n*-BA-0.1, was conveniently obtained by using the same preAPCN, PFPA-0.1, but reacting the PFPA active ester with *n*-BA under similar conditions. To ensure that both samples possess the same swelling capability, we incubated the conetworks into PBS buffer and determined the degree of swelling. Both conetworks showed very similar S_{Vol} with 1.48 ± 0.04 for Biotin-0.1 and 1.46 ± 0.02 for *n*-BA-0.1. To load the conetworks with protein, they were incubated in a 0.5 mg mL^{-1} solution of AlexaFluor488-labeled streptavidin in PBS buffer for one night at room temperature. To characterize the leaching of the protein out of the APCNs, they were subsequently transferred into fresh PBS buffer. The samples were washed in PBS buffer over several days with an exchange of buffer solution before each analysis steps. The APCNs were analyzed together using a microarray fluorescence scanner. A fluorescence scanning image after two days of washing is presented in **Figure 6b**. For Biotin-0.1, strong fluorescence was found compared to the control *n*-BA-0.1, which shows only little fluorescence due to a non-specific adsorption, which has been reported before.³³ Fluorescence emission spectra obtained with a fluorescence spectrophotometer confirm the difference in protein adsorption (**Figure 6c**). Biotin-0.1 has a much stronger emission peak around 520 nm than the control sample. To

compare the two APCNs quantitatively, the average fluorescent emission intensities over a representative area of the APCNs was measured. The ratio between the area average emission intensities $I_{biotin}/I_{control}$ during the leaching experiment is plotted in **Figure 6d**. Already after the loading step, the fluorescence of Biotin-0.1 was more than two times stronger than the fluorescence of the control, indicating that the specific binding of streptavidin to biotin enriched the protein within the APCN. The ratio $I_{biotin}/I_{control}$ increased further with washing of the APCNs in PBS buffer for 2 days, indicating that the non-specifically loaded streptavidin in the control sample mostly washed out, while Biotin-0.1 retained its protein load. Longer washing slightly reduced the fluorescence ratio between the two samples. Nevertheless, even after more than a month of washing Biotin-0.1 retained most of its protein cargo.

CONCLUSIONS

The fabrication of APCNs is faced by the central challenge of combining immiscible polymers into a macroscopically homogeneous, crosslinked material. To address this miscibility challenge, we presented a strategy for the synthesis of APCNs based on PFPA. With its dual role of providing miscibility with hydrophobic macromer crosslinkers and other hydrophobized monomers as well as providing active ester functionality, it acts as a hydrophobically masked *N*-alkyl acrylamide. Therefore, after the polymerization, the networks could be easily transformed into almost any kind of poly(*N*-alkyl acrylamide)-based APCN. These APCNs can be accurately designed by controlling the functionality of the *N*-alkyl acrylamide units in order to tailor the material properties according to any specific applications. Furthermore, the combination of PFPA with other masked monomers, such as TMS-HEA, allows the homogenous incorporation of functional groups, including pH-responsive moieties, fluorescent dyes and protein binding motives, in precisely defined amounts into the hydrophilic phase of the APCNs. The wealth of

available functionalities from an active ester-based approach introduces a previously unavailable range, versatility and control to the fabrication and functionalization of APCNs. We expect our synthesis strategy to lead to an increased understanding of the influence of the ACPN's network structure and chemical functionality on their performance. Most importantly, however, it will allow the fabrication of novel functional APCNs, which could find applications in drug delivery, for functional contact lenses, sensors, membranes, self-healing materials and for interfacial biocatalysis.

ASSOCIATED CONTENT

Additional experimental details and analytical data are provided in the supporting information. This material is available free of charge via the Internet at <http://pubs.acs.org>.

AUTHOR INFORMATION

Corresponding Author

* E-mail: Luciano.boesel@empa.ch

* E-Mail: nico.bruns@unifr.ch

Author Contributions

The manuscript was written through contributions of all authors. All authors have given approval to the final version of the manuscript.

ACKNOWLEDGMENT

The Swiss National Science Foundation (SNSF) is acknowledged for the financial support to LFB through Grant No. 200021_172609 (“Teleflow”), to financial support to N.B. through Grant No. PP00P2_144697 and PP00P2_172927 and to support to the NMR hardware through Grant No. 206021_150638/1. We thank Dr. Fabrizio Spano (Empa) and Dr. Christian Bippes (Nanosurf AG, Switzerland) for support with AFM measurements. We thank Dr. Dorina Opris and Beatrice Fischer (both Empa) for GPC measurements. We thank Dr. Daniel Rentsch (Empa) for the NMR measurement. We thank Dr. James R. Hemmer (U.S. Naval Research Laboratory), Dr. Clément Mugemana (Luxembourg Institute of Science and Technology), Dr. Riccardo Innocenti Malini (Empa), and Lea Oberhänsli (Empa) for their support.

REFERENCES

1. Schacher, F. H.; Rugar, P. A.; Manners, I. Functional Block Copolymers: Nanostructured Materials with Emerging Applications. *Angew. Chem. Int. Ed.* **2012**, *51* (32), 7898-7921.
2. Patrickios, C. S.; Georgiou, T. K. Covalent amphiphilic polymer networks. *Curr. Opin. Colloid Interface Sci.* **2003**, *8* (1), 76-85.
3. Erdodi, G.; Kennedy, J. P. Amphiphilic conetworks: Definition, synthesis, applications. *Prog. Polym. Sci.* **2006**, *31* (1), 1-18.
4. Mespouille, L.; Hedrick, J. L.; Dubois, P. Expanding the role of chemistry to produce new amphiphilic polymer (co)networks. *Soft Matter* **2009**, *5* (24), 4878-4892.
5. Nicolson, P. C.; Vogt, J. Soft contact lens polymers: an evolution. *Biomaterials* **2001**, *22* (24), 3273-3283.

6. Tighe, B. J. A Decade of Silicone Hydrogel Development: Surface Properties, Mechanical Properties, and Ocular Compatibility. *Eye & Contact Lens-Science and Clinical Practice* **2013**, *39* (1), 4-12.
7. Isayeva, I. S.; Kasibhatla, B. T.; Rosenthal, K. S.; Kennedy, J. P. Characterization and performance of membranes designed for macroencapsulation/implantation of pancreatic islet cells. *Biomaterials* **2003**, *24* (20), 3483-3491.
8. Tiller, J. C.; Sprich, C.; Hartmann, L. Amphiphilic conetworks as regenerative controlled releasing antimicrobial coatings. *J. Controlled Release* **2005**, *103* (2), 355-367.
9. Kang, J.; Erdodi, G.; Kennedy, J. P.; Chou, H.; Lu, L.; Grundfest-Broniatowski, S. Toward a Bioartificial Pancreas: Diffusion of Insulin and IgG Across Immunoprotective Membranes with Controlled Hydrophilic Channel Diameters. *Macromol. Biosci.* **2010**, *10* (4), 369-377.
10. Guzman, G.; Es-haghi, S. S.; Nugay, T.; Cakmak, M. Zero-Order Antibiotic Release from Multilayer Contact Lenses: Nonuniform Drug and Diffusivity Distributions Produce Constant-Rate Drug Delivery. *Adv. Healthcare Mater.* **2017**, *6* (3), 1600775.
11. Chandel, A. K. S.; Kumar, C. U.; Jewrajka, S. K. Effect of Polyethylene Glycol on Properties and Drug Encapsulation -Release Performance of Biodegradable/Cytocompatible Agarose-Polyethylene Glycol Polycaprolactone Amphiphilic Co-Network Gels. *ACS Appl. Mater. Interfaces* **2016**, *8* (5), 3182-3192.

12. Shi, L.; Xie, P.; Li, Z. M.; Wu, Y. P.; Deng, J. P. Chiral pH-Responsive Amphiphilic Polymer Co-networks: Preparation, Chiral Recognition, and Release Abilities. *Macromol. Chem. Phys.* **2013**, *214* (12), 1375-1383.
13. Lin, C.; Gitsov, I. Preparation and Characterization of Novel Amphiphilic Hydrogels with Covalently Attached Drugs and Fluorescent Markers. *Macromolecules* **2010**, *43* (23), 10017-10030.
14. Gu, D.; Tan, S.; O'Connor, A. J.; Qiao, G. G. On-Demand Cascade Release of Hydrophobic Chemotherapeutics from a Multicomponent Hydrogel System. *ACS Biomater. Sci. Eng.* **2018**, *4* (5), 1696-1707.
15. Iván, B.; Kennedy, J. P.; Mackey, P. W. Amphiphilic networks. Synthesis and characterization of and drug release from poly(2-hydroxyethyl methacrylate)-1-polyisobutylene. In *ACS Symp. Ser.*, American Chemical Society: Washington, DC, 1991; Vol. 469, pp 203-212.
16. Iván, B.; Kennedy, J. P.; Mackey, P. W. Amphiphilic Networks - Synthesis and Characterization of and Drug Release from Poly(N,N-dimethylacrylamide)-1-polyisobutylene. In *ACS Symp. Ser.*, American Chemical Society: Washington, DC, 1991; Vol. 469, pp 194-202.
17. Pollack, K. A.; Imbesi, P. M.; Raymond, J. E.; Wooley, K. L. Hyperbranched Fluoropolymer-Polydimethylsiloxane-Poly(ethylene glycol) Cross-Linked Terpolymer Networks Designed for Marine and Biomedical Applications: Heterogeneous Nontoxic Antibiofouling Surfaces. *ACS Appl. Mater. Interfaces* **2014**, *6* (21), 19265-19274.

18. Wang, H. Y.; Jasensky, J.; Ulrich, N. W.; Cheng, J. J.; Huang, H.; Chen, Z.; He, C. J. Capsaicin-Inspired Thiol-Ene Terpolymer Networks Designed for Antibiofouling Coatings. *Langmuir* **2017**, *33* (47), 13689-13698.
19. Wang, Y.; Betts, D. E.; Finlay, J. A.; Brewer, L.; Callow, M. E.; Callow, J. A.; Wendt, D. E.; DeSimone, J. M. Photocurable Amphiphilic Perfluoropolyether/Poly(ethylene glycol) Networks for Fouling-Release Coatings. *Macromolecules* **2011**, *44* (4), 878-885.
20. Du Prez, F. E.; Goethals, E. J.; Schue, R.; Qariouh, H.; Schue, F. Segmented network structures for the separation of water/ethanol mixtures by pervaporation. *Polym. Int.* **1998**, *46* (2), 117-125.
21. Li, X.; Basko, M.; Du Prez, F.; Vankelecom, I. F. J. Multifunctional Membranes for Solvent Resistant Nanofiltration and Pervaporation Applications Based on Segmented Polymer Networks. *J. Phys. Chem. B* **2008**, *112* (51), 16539-16545.
22. Tobis, J.; Boch, L.; Thomann, Y.; Tiller, J. C. Amphiphilic polymer conetworks as chiral separation membranes. *J. Membr. Sci.* **2011**, *372* (1-2), 219-227.
23. Guzman, G.; Nugay, T.; Nugay, I.; Nugay, N.; Kennedy, J.; Cakmak, M. High Strength Bimodal Amphiphilic Conetworks for Immunoisolation Membranes: Synthesis, Characterization, and Properties. *Macromolecules* **2015**, *48* (17), 6251-6262.
24. Walker, C. N.; Versek, C.; Touminen, M.; Tew, G. N. Tunable Networks from Thiolenes Chemistry for Lithium Ion Conduction. *ACS Macro Lett.* **2012**, *1* (6), 737-741.

25. Walker, C. N.; Bryson, K. C.; Hayward, R. C.; Tew, G. N. Wide Bicontinuous Compositional Windows from Co-Networks Made with Telechelic Macromonomers. *Acs Nano* **2014**, *8* (12), 12376-12385.
26. McLeod, K. R.; Tew, G. N. Microphase-Separated Thiol–Ene Conetworks from Telechelic Macromonomers with Asymmetric Molecular Weights. *Macromolecules* **2017**.
27. Hanco, M.; Bruns, N.; Rentmeister, S.; Tiller, J. C.; Heinze, J. Nanophase-Separated Amphiphilic Conetworks as Versatile Matrixes for Optical Chemical and Biochemical Sensors. *Anal. Chem.* **2006**, *78* (18), 6376-6383.
28. Hanco, M.; Bruns, N.; Tiller, J. C.; Heinze, J. Optical biochemical sensor for determining hydroperoxides in nonpolar organic liquids as archetype for sensors consisting of amphiphilic conetworks as immobilisation matrices. *Anal. Bioanal. Chem.* **2006**, *386* (5), 1273-1283.
29. Meskath, S.; Urban, G.; Heinze, J. A new optochemical chlorine gas sensor based on the application of amphiphilic co-networks as matrices. *Sens. Actuators, B* **2011**, *151* (2), 327-332.
30. Meskath, S.; Urban, G.; Heinze, J. Nanophase separated amphiphilic polymer co-networks as efficient matrices for optical sensors: Rapid and sensitive detection of NO₂. *Sens. Actuators, B* **2013**, *186*, 367-373.
31. Scholler, K.; Toncelli, C.; Experton, J.; Widmer, S.; Rentsch, D.; Vetushka, A.; Martin, C. J.; Heuberger, M.; Housecroft, C. E.; Constable, E. C.; Boesel, L. F.; Scherer, L. J. 2,2',6',2''-Terpyridine-functionalized redox-responsive hydrogels as a platform for multi responsive amphiphilic polymer membranes. *RSC Adv.* **2016**, *6* (100), 97921-97930.

32. Rother, M.; Barmettler, J.; Reichmuth, A.; Araujo, J. V.; Rytka, C.; Glaied, O.; Pieles, U.; Bruns, N. Self-Sealing and Puncture Resistant Breathable Membranes for Water-Evaporation Applications. *Adv. Mater.* **2015**, *27* (42), 6620-6624.
33. Bruns, N.; Tiller, J. C. Amphiphilic Network as Nanoreactor for Enzymes in Organic Solvents. *Nano Lett.* **2005**, *5* (1), 45-48.
34. Savin, G.; Bruns, N.; Thomann, Y.; Tiller, J. C. Nanophase Separated Amphiphilic Microbeads. *Macromolecules* **2005**, *38* (18), 7536-7539.
35. Bruns, N.; Bannwarth, W.; Tiller, J. C. Amphiphilic conetworks as activating carriers for the enhancement of enzymatic activity in supercritical CO₂. *Biotechnol. Bioeng.* **2008**, *101* (1), 19-26.
36. Schoenfeld, I.; Dech, S.; Ryabenky, B.; Daniel, B.; Glowacki, B.; Ladisch, R.; Tiller, J. C. Investigations on diffusion limitations of biocatalyzed reactions in amphiphilic polymer conetworks in organic solvents. *Biotechnol. Bioeng.* **2013**, *110* (9), 2333-2342.
37. Sittko, I.; Kremser, K.; Roth, M.; Kuehne, S.; Stuhr, S.; Tiller, J. C. Amphiphilic polymer conetworks with defined nanostructure and tailored swelling behavior for exploring the activation of an entrapped lipase in organic solvents. *Polymer* **2015**, *64*, 122-129.
38. Scheibel, D. M.; Gitsov, I. Polymer-Assisted Biocatalysis: Effects of Macromolecular Architectures on the Stability and Catalytic Activity of Immobilized Enzymes toward Water-Soluble and Water-Insoluble Substrates. *ACS Omega* **2018**, *3* (2), 1700-1709.
39. Schöllner, K.; Küpfer, S.; Baumann, L.; Hoyer, P. M.; de Courten, D.; Rossi, R. M.; Vetushka, A.; Wolf, M.; Bruns, N.; Scherer, L. J. From Membrane to Skin: Aqueous Permeation

Control Through Light-Responsive Amphiphilic Polymer Co-Networks. *Adv. Funct. Mater.* **2014**, *24* (33), 5194-5201.

40. Yuan, Y.; Zhang, A.-K.; Ling, J.; Yin, L.-H.; Chen, Y.; Fu, G.-D. Well-defined biodegradable amphiphilic conetworks. *Soft Matter* **2013**, *9* (27), 6309-6318.

41. Xu, J. F.; Qiu, M.; Ma, B. M.; He, C. J. "Near Perfect" Amphiphilic Conetwork Based on End-Group Cross-Linking of Polydimethylsiloxane Triblock Copolymer via Atom Transfer Radical Polymerization. *ACS Appl. Mater. Interfaces* **2014**, *6* (17), 15283-15290.

42. Kepola, E. J.; Loizou, E.; Patrickios, C. S.; Leontidis, E.; Voutouri, C.; Stylianopoulos, T.; Schweins, R.; Gradzielski, M.; Krumm, C.; Tiller, J. C.; Kushnir, M.; Wesdemiotis, C. Amphiphilic Polymer Conetworks Based on End-Linked "Core-First" Star Block Copolymers: Structure Formation with Long-Range Order. *ACS Macro Letters* **2015**, *4* (10), 1163-1168.

43. Hiroi, T.; Kondo, S.; Sakai, T.; Gilbert, E. P.; Han, Y. S.; Kim, T. H.; Shibayama, M. Fabrication and Structural Characterization of Module-Assembled Amphiphilic Conetwork Gels. *Macromolecules* **2016**, *49* (13), 4940-4947.

44. Kitiri, E.; Patrickios, C.; Voutouri, C.; Stylianopoulos, T.; Hoffmann, I.; Schweins, R.; Gradzielski, M. Synthesis and Characterization of Double-networks Based on pH-responsive, Amphiphilic "Core-first" Star First Polymer Conetworks Prepared by Sequential RAFT Polymerization. *Polym. Chem.* **2016**, 245-259.

45. Ohashi, R.; Bartels, J. W.; Xu, J. Q.; Wooley, K. L.; Schaefer, J. Solid-State NMR Investigations of the Unusual Effects Resulting from the Nanoconfinement of Water within Amphiphilic Crosslinked Polymer Networks. *Adv. Funct. Mater.* **2009**, *19* (21), 3404-3410.

46. Gitsov, I.; Zhu, C. Novel Functionally Grafted Pseudo-Semi-interpenetrating Networks Constructed by Reactive Linear–Dendritic Copolymers1. *J. Am. Chem. Soc.* **2003**, *125* (37), 11228-11234.
47. Hu, Z.; Chen, L.; Betts, D. E.; Pandya, A.; Hillmyer, M. A.; DeSimone, J. M. Optically Transparent, Amphiphilic Networks Based on Blends of Perfluoropolyethers and Poly(ethylene glycol). *J. Am. Chem. Soc.* **2008**, *130* (43), 14244-14252.
48. Zhou, C.; Qian, S. S.; Zhang, A. K.; Xu, L. Q.; Zhu, J.; Cheng, Z. P.; Kang, E. T.; Yao, F.; Fu, G. D. A well-defined amphiphilic polymer co-network from precise control of the end-functional groups of linear RAFT polymers. *RSC Adv.* **2014**, *4* (16), 8144-8156.
49. Apostolides, D. E.; Patrickios, C. S.; Sakai, T.; Guerre, M.; Lopez, G.; Améduri, B.; Ladmiral, V.; Simon, M.; Gradzielski, M.; Clemens, D.; Krumm, C.; Tiller, J. C.; Ernould, B.; Gohy, J.-F. Near-Model Amphiphilic Polymer Conetworks Based on Four-Arm Stars of Poly(vinylidene fluoride) and Poly(ethylene glycol): Synthesis and Characterization. *Macromolecules* **2018**, *51* (7), 2476-2488.
50. Erdodi, G.; Iván, B. Novel amphiphilic conetworks composed of telechelic poly(ethylene oxide) and three-arm star polyisobutylene. *Chem. Mater.* **2004**, *16* (6), 959-962.
51. Kali, G.; Georgiou, T. K.; Iván, B.; Patrickios, C. S.; Loizou, E.; Thomann, Y.; Tiller, J. C. Synthesis and Characterization of Anionic Amphiphilic Model Conetworks Based on Methacrylic Acid and Methyl Methacrylate: Effects of Composition and Architecture. *Macromolecules* **2007**, *40* (6), 2192-2200.

52. Kali, G.; Georgiou, T. K.; Iván, B.; Patrickios, C. S. Anionic Amphiphilic End-Linked Conetworks by the Combination of Quasiliving Carbocationic and Group Transfer Polymerizations. *J. Polym. Sci., Part A: Polym. Chem.* **2009**, *47* (17), 4289-4301.
53. Rikkou-Kalourkoti, M.; Patrickios, C. S. Synthesis and Characterization of End-Linked Amphiphilic Copolymer Conetworks Based on a Novel Bifunctional Cleavable Chain Transfer Agent. *Macromolecules* **2012**, *45* (19), 7890-7899.
54. Rikkou-Kalourkoti, M.; Kitiri, E. N.; Patrickios, C. S.; Leontidis, E.; Constantinou, M.; Constantinides, G.; Zhang, X. H.; Papadakis, C. M. Double Networks Based on Amphiphilic Cross-Linked Star Block Copolymer First Conetworks and Randomly Cross-Linked Hydrophilic Second Networks. *Macromolecules* **2016**, *49* (5), 1731-1742.
55. Achilleos, D. S.; Georgiou, T. K.; Patrickios, C. S. Amphiphilic Model Conetworks Based on Cross-Linked Star Copolymers of Benzyl Methacrylate and 2-(Dimethylamino)ethyl Methacrylate: Synthesis, Characterization, and DNA Adsorption Studies. *Biomacromolecules* **2006**, *7* (12), 3396-3405.
56. Georgiou, T. K.; Patrickios, C. S.; Groh, P. W.; Iván, B. Amphiphilic model conetworks of polyisobutylene methacrylate and 2-(dimethylamino)ethyl methacrylate prepared by the combination of quasiliving carbocationic and group transfer polymerizations. *Macromolecules* **2007**, *40* (7), 2335-2343.
57. Pásztor, S.; Iván, B.; Kali, G. Extreme difference of polarities in a single material: Poly(acrylic acid)-based amphiphilic conetworks with polyisobutylene cross-linker. *J. Polym. Sci., Part A: Polym. Chem.* **2017**, *55* (11), 1818-1821.

58. Bruns, N.; Scherble, J.; Hartmann, L.; Thomann, R.; Iván, B.; Mülhaupt, R.; Tiller, J. C. Nanophase Separated Amphiphilic Conetwork Coatings and Membranes. *Macromolecules* **2005**, *38* (6), 2431-2438.
59. Tironi, C. N.; Graf, R.; Lieberwirth, I.; Klapper, M.; Mullen, K. Synthesis and Selective Loading of Polyhydroxyethyl Methacrylate-/Polysulfone Amphiphilic Polymer Conetworks. *ACS Macro Lett.* **2015**, *4* (11), 1302-1306.
60. Domjan, A.; Erdodi, G.; Wilhelm, M.; Neidhofer, M.; Landfester, K.; Iván, B.; Spiess, H. W. Structural studies of nanophase-separated poly(2-hydroxyethyl methacrylate)-*l*-polyisobutylene amphiphilic conetworks by solid-state NMR and small-angle x-ray scattering. *Macromolecules* **2003**, *36* (24), 9107-9114.
61. Scherble, J.; Thomann, R.; Iván, B.; Mülhaupt, R. Formation of CdS nanoclusters in phase-separated poly(2-hydroxyethyl methacrylate)-*l*-polyisobutylene amphiphilic conetworks. *J. Polym. Sci., Part B: Polym. Phys.* **2001**, *39* (12), 1429-1436.
62. Kali, G.; Iván, B. Poly(methacrylic acid)-*l*-Polyisobutylene Amphiphilic Conetworks by Using an Ethoxyethyl-Protected Comonomer: Synthesis, Protecting Group Removal in the Cross-Linked State, and Characterization. *Macromol. Chem. Phys.* **2015**, *216* (6), 605-613.
63. Bruns, N.; Tiller, J. C. Nanophasic Amphiphilic Conetworks with a Fluorophilic Phase. *Macromolecules* **2006**, *39* (13), 4386-4394.
64. Fodor, C.; Kali, G.; Iván, B. Poly(N-vinylimidazole)-*l*-Poly(tetrahydrofuran) Amphiphilic Conetworks and Gels: Synthesis, Characterization, Thermal and Swelling Behavior. *Macromolecules* **2011**, *44* (11), 4496-4502.

65. Kali, G.; Vavra, S.; Laszlo, K.; Iván, B. Thermally Responsive Amphiphilic Conetworks and Gels Based on Poly(N-isopropylacrylamide) and Polyisobutylene. *Macromolecules* **2013**, *46* (13), 5337-5344.
66. Fodor, C.; Kali, G.; Thomann, R.; Thomann, Y.; Iván, B.; Mülhaupt, R. Nanophasic morphologies as a function of the composition and molecular weight of the macromolecular cross-linker in poly(N-vinylimidazole)-I-poly(tetrahydrofuran) amphiphilic conetworks: bicontinuous domain structure in broad composition ranges. *RSC Adv.* **2017**, *7* (12), 6827-6834.
67. Fan, X.; Wang, M.; Yuan, D.; He, C. Amphiphilic Conetworks and Gels Physically Cross-Linked via Stereocomplexation of Polylactide. *Langmuir* **2013**, *29* (46), 14307-14313.
68. Haraszti, M.; Tóth, E.; Iván, B. Poly(methacrylic acid)-I-Polyisobutylene: A Novel Polyelectrolyte Amphiphilic Conetwork. *Chem. Mater.* **2006**, *18* (20), 4952-4958.
69. Das, A.; Théato, P. Activated Ester Containing Polymers: Opportunities and Challenges for the Design of Functional Macromolecules. *Chem. Rev.* **2015**, *116* (3), 1434-1495.
70. Eberhardt, M.; Mruk, R.; Zentel, R.; Théato, P. Synthesis of pentafluorophenyl(meth)acrylate polymers: New precursor polymers for the synthesis of multifunctional materials. *Eur. Polym. J.* **2005**, *41* (7), 1569-1575.
71. Das, A.; Théato, P. Multifaceted Synthetic Route to Functional Polyacrylates by Transesterification of Poly(pentafluorophenyl acrylates). *Macromolecules* **2015**, *48* (24), 8695-8707.

72. Jochum, F. D.; Théato, P. Temperature and light sensitive copolymers containing azobenzene moieties prepared via a polymer analogous reaction. *Polymer* **2009**, *50* (14), 3079-3085.
73. Ramireddy, R. R.; Prasad, P.; Finne, A.; Thayumanavan, S. Zwitterionic amphiphilic homopolymer assemblies. *Polym. Chem.* **2015**, *6* (33), 6083-6087.
74. Kubilis, A.; Abdulkarim, A.; Eissa, A. M.; Cameron, N. R. Giant Polymersome Protocells Dock with Virus Particle Mimics via Multivalent Glycan-Lectin Interactions. *Scientific Reports* **2016**, *6*, 32414.
75. Zhuang, J. M.; Jiwanich, S.; Deepak, V. D.; Thayumanavan, S. Facile Preparation of Nanogels Using Activated Ester Containing Polymers. *ACS Macro Lett.* **2012**, *1* (1), 175-179.
76. Liu, Y. L.; Pauloehrl, T.; Presolski, S. I.; Albertazzi, L.; Palmans, A. R. A.; Meijer, E. W. Modular Synthetic Platform for the Construction of Functional Single-Chain Polymeric Nanoparticles: From Aqueous Catalysis to Photosensitization. *J. Am. Chem. Soc.* **2015**, *137* (40), 13096-13105.
77. Das, A.; Lin, S.; Théato, P. Supramolecularly Cross-Linked Nanogel by Merocyanine Pendent Copolymer. *ACS Macro Lett.* **2016**, 50-55.
78. Kessler, D.; Théato, P. Reactive Surface Coatings Based on Polysilsesquioxanes: Defined Adjustment of Surface Wettability. *Langmuir* **2009**, *25* (24), 14200-14206.
79. Seo, J.; Schattling, P.; Lang, T.; Jochum, F.; Nilles, K.; Théato, P.; Char, K. Covalently Bonded Layer-by-Layer Assembly of Multifunctional Thin Films Based on Activated Esters. *Langmuir* **2010**, *26* (3), 1830-1836.

80. Choi, J.; Schattling, P.; Jochum, F. D.; Pyun, J.; Char, K.; Théato, P. Functionalization and patterning of reactive polymer brushes based on surface reversible addition and fragmentation chain transfer polymerization. *J. Polym. Sci., Part A: Polym. Chem.* **2012**, *50* (19), 4010-4018.
81. Arnold, R. M.; McNitt, C. D.; Popik, V. V.; Locklin, J. Direct grafting of poly(pentafluorophenyl acrylate) onto oxides: versatile substrates for reactive microcapillary printing and self-sorting modification. *Chem. Commun.* **2014**, *50* (40), 5307-5309.
82. Ulrich, S.; Hemmer, J. R.; Page, Z. A.; Dolinski, N. D.; Rifaie-Graham, O.; Bruns, N.; Hawker, C. J.; Boesel, L. F.; Read de Alaniz, J. Visible Light-Responsive DASA-Polymer Conjugates. *ACS Macro Lett.* **2017**, *6* (7), 738-742.
83. Rifaie-Graham, O.; Ulrich, S.; Galensowske, N. F. B.; Balog, S.; Chami, M.; Rentsch, D.; Hemmer, J. R.; Read de Alaniz, J.; Boesel, L. F.; Bruns, N. Wavelength-Selective Light-Responsive DASA-Functionalized Polymersome Nanoreactors. *J. Am. Chem. Soc.* **2018**.
84. Britton, H. T. S.; Robinson, R. A. CXCVIII.-Universal buffer solutions and the dissociation constant of veronal. *J. Chem. Soc.* **1931**, (0), 1456-1462.
85. Glatter, O. A new method for the evaluation of small-angle scattering data. *J. Appl. Crystallogr.* **1977**, *10* (5), 415-421.
86. Fritz, G.; Bergmann, A.; Glatter, O. Evaluation of small-angle scattering data of charged particles using the generalized indirect Fourier transformation technique. *J. Chem. Phys.* **2000**, *113* (21), 9733-9740.

87. Beija, M.; Li, Y.; Lowe, A. B.; Davis, T. P.; Boyer, C. Factors influencing the synthesis and the post-modification of PEGylated pentafluorophenyl acrylate containing copolymers. *Eur. Polym. J.* **2013**, *49* (10), 3060-3071.
88. McLean, R. S.; Sauer, B. B. Tapping-Mode AFM Studies Using Phase Detection for Resolution of Nanophases in Segmented Polyurethanes and Other Block Copolymers. *Macromolecules* **1997**, *30* (26), 8314-8317.
89. Zhang, X. H.; Kyriakos, K.; Rikkou-Kalourkoti, M.; Kitiri, E. N.; Patrickios, C. S.; Papadakis, C. M. Amphiphilic single and double networks: a small-angle X-ray scattering investigation. *Colloid. Polym. Sci.* **2016**, *294* (6), 1027-1036.
90. Zeng, D.; Ribbe, A.; Hayward, R. C. Anisotropic and Interconnected Nanoporous Materials from Randomly End-Linked Copolymer Networks. *Macromolecules* **2017**, *50* (12), 4668-4676.
91. Schwab, M.; Stühn, B. Asymmetric diblock copolymers-phase behaviour and kinetics of structure formation. *Colloid. Polym. Sci.* **1997**, *275* (4), 341-351.
92. Ndoni, S.; Vigild, M. E.; Berg, R. H. Nanoporous materials with spherical and gyroid cavities created by quantitative etching of polydimethylsiloxane in polystyrene-polydimethylsiloxane block copolymers. *J. Am. Chem. Soc.* **2003**, *125* (44), 13366-13367.
93. Carey, F. *Organic Chemistry*. 5th ed.; McGraw-Hill Education: New York City, 2002, p 1059.
94. Dech, S.; Wruk, V.; Fik, C. P.; Tiller, J. C. Amphiphilic polymer conetworks derived from aqueous solutions for biocatalysis in organic solvents. *Polymer* **2012**, *53* (3), 701-707.

95. Kessler, D.; Roth, P. J.; Théato, P. Reactive Surface Coatings Based on Polysilsesquioxanes: Controlled Functionalization for Specific Protein Immobilization. *Langmuir* **2009**, *25* (17), 10068-10076.

TOC graphic

Wide Range of Functionalized Poly(*N*-alkyl acrylamide)-based Amphiphilic Polymer Conetworks via Active Ester Precursors

Sebastian Ulrich, Amin Sadeghpour, René M. Rossi, Nico Bruns,* Luciano F. Boesel*

